Generalized Incremental Predictive Filter for Integrated Navigation System INS/GPS in Tangent Frame

Nemat Allah Ghahremani[1]* and Hassan Majed Alhassan[2]

[1] Faculty of Electrical & Computer engineering, Malek Ashtar University of Technology, Tehran, Iran. (e-mail: Ghahremani @mut.ac.ir).

[2] Faculty of Electrical & Computer engineering, Malek Ashtar University of Technology, Tehran, Iran. (e-mail: hassan.majed.alhassan@gmail.com)

*Corresponding Author

Received 26 Nov 2021 Received in revised form 27 Feb 2022 Accepted 8 Apr 2022

Type of Article: Research paper

***Abstract*- The extended Kalman filter (EKF) is a widely used algorithm for nonlinear estimation of Inertial Navigation Systems (INS) and the Global Position System (GPS) integration. However, EKF has several limitations, such as linearization dependency, and the model error statistics are assumed as a zero-mean Gaussian noise with known covariance. Consequently, if EKF is not tuned correctly, the INS error predictions can quickly diverge.**

To overcome the limitations of existing Kalman algorithms, this paper derives a real-time predictive approach. The proposed method increases the accuracy and the reliability requirements of loosely INS/GPS integration by estimating the unknown model errors of sensors without augmenting the state space. Also, considering the insufficiency of the researches on the integrated navigation in tangent (launch) frame, this research derives the navigation equations in tangent frame and its error model is analyzed. The estimation performance of the predictive approach is analyzed.

The performance is verified using an experimental data acquired from a land-vehicle test. The results of predictive filter demonstrate superior performance to the traditional EKF. The test results of land-vehicle navigation validate the advantages of the presented method, which increases the position accuracy by an amount of 70% and it decreases the computational cost to 50% and improves the estimation performance for the integrated INS/GPS better than the traditional EKF. This test is a fundamental step to determine the capability of the filter for robotics and aerospace applications in future.

***Keywords*: Extended Kalman filter, Incremental predictive filter, INS/GPS, Land-vehicle test, Tangent frame.**

I. INTRODUCTION

TO interpret the necessity of the new predictive filtering method for integrated INS/GPS, this section reviews the state of the art of INS/GNSS integration regarding the principles of inertial navigation and the most common estimation methods for inertial navigation. With the rapid development of strap-down inertial navigation systems based on micro-electro-mechanical systems (MEMS) technology, as well as the regular improvement of the global navigation satellite system (GNSS), the INS combines with the GNSS to improve the precision of navigation systems [1]. The integrated navigation systems are used in different navigation applications, such as land vehicle navigation applications, robotics [2], missiles guidance [3-5], and reconnaissance aircraft. The INS/GPS integration has many designs [6-11], that depends on the application's nature which uses the integrated navigation [12]. This variety of solutions comes actually from the architecture of the integration [13]. There are three main architectures of INS/GPS integration, namely loosely, tightly and ultra-tightly couplings [7, 10, 14]. The loosely architecture is the more common integration techniques [7]. In the loosely-coupled architecture the GPS solution (position and velocity) is merged with the inertial based information to obtain the final output of the integrated system.

Traditionally, the outputs from INS sensors and GPS are combined using the EKF [15] or other alternative KF algorithms [16]; to produce the best estimate of the actual vehicle states. Recently, there exist several classes of research concerning INS/GPS filtering methods for integrated navigation. The filtering methods can be categorized as follows: the minimum mean-square error (MMSE) based methods, such as the extended Kalman filter (EKF) [17], the sampling-based methods, such as the unscented Kalman filter (UKF) [9]and particle filters

[DOI: 10.52547/jocee.1.1.49]

(PF) [18], the artificial intelligence methods (AI) [19], such as the artificial neural networks or the adaptive neuro-fuzzy inference systems (ANFIS) [20], and the predictive filtering or model predictive filtering (MPF) [21] to track measurement output by using prediction output to estimate model error of the system. Also, there are some recent researches use the adaptive Kalman filter (AKF) for INS/GPS integration [22, 23]. The AKF adjusts the value of the noise covariance matrices for the system (Q) and measurement (R) only, therefore, the AKF is not robust to model error.

The extended KF plays the principal role in estimation and navigation software design and it has been widely applied in navigation applications [24-26]. However, EKF assume that true system model is known with certainty and EKF uses the Taylor series expansion on the nonlinear system equations and takes the first-order terms to provide a suitable solution to some extent with nonlinearities. Therefore, the EKF is not optimal filter (as KF) for solving the problem of nonlinear system state estimation and cannot guarantee the estimation stability. Compared with other nonlinear filter methods, predicative filter can estimate model error, so it has developed rapidly [27-29]. The applications of the MPF have been reported in various fields such as navigation, attitude determination[30, 31]. The conventional predictive filter, due to the use of Lie derivatives in its formulation [32], has a very complex mathematical algorithm. Its complexity makes the design of the predictive filter a very time-consuming and inflexible process [33].

The main objective of this research is optimizing the estimation procedure of the INS/GPS integrated system by replacing the conventional EKF formulation of the integration by an incremental predictive one. The new real-time algorithm named generalized incremental predictive Kalman filter (GIP_KF) is superior to the EKF as it provides a means to accommodate irregular situation. This enhances the reliability and accuracy of the integrated INS/GPS in kinematic applications. To achieve the goal of this research, verification of the proposed algorithm is performed in tangent frame both by using real navigation data for ground vehicle. A thorough analysis is carried out to show the effectiveness and suitability of the predictive technique. It is shown that the GIP_KF is outperforms the EKF and it has potential for navigation applications requiring high reliability and accuracy.

The remainder of this paper is structured as follows: Section 2 presents the derivation of INS/GPS mechanization in tangent frame. Section 3 covers the predictive filtering theory and implementation for INS/GPS integrated system. The equivalent model error is derived for INS systems, and then the derivation of the incremental predictive filter is given in details. Section 4 explores a comparative INS/GPS integration using GIP_KF and EKF. Also, it provides the results of the experimental testes. Finally, section 5 summarizes the work done in this research and concludes the major results and findings.

II. INS/GPS Integration in Tangent Frame

The tangent frame (t-frame) is considered stationary relative to the center of the rotating earth since the origin of coordinates does not move with the vehicle but rather remains fixed at the point of initialization (at start time t0). In this case, while the IMU moves with the vehicle, its orientation relative to the earth remains fixed at its initial value (see Fig. 1). Therefore, this frame is a good reference frame to navigation calculations.

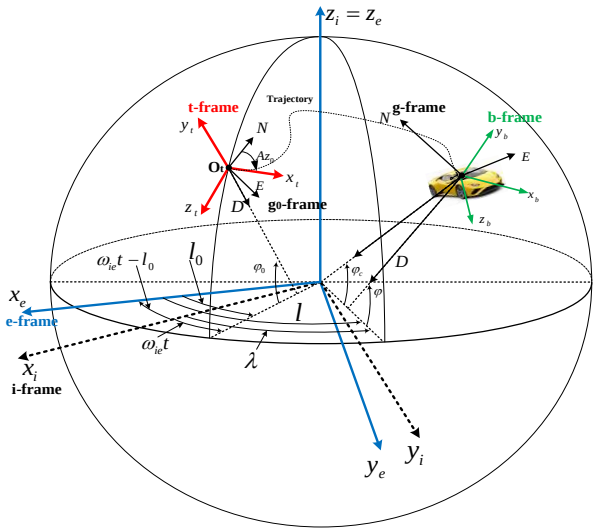

Fig. 1. The tangent frame, Body Frame Geodetic, ECEF, and local NED coordinate systems for terrestrial vehicle

The t-frame takes advantage of the fact that constant IMU rates can be precisely determined at start-up. t-frame is usually employed when the travelled distance is limited. The tangent frame is also known as the launch point inertial frame (LPI) [34], or launch-centered earth-fixed (LCEF) frame [35-38]. Some kinds of literature confused between the local-level frame and tangent frame, for example, [39] define the l-frame as the tangent plane reference system. So our tangent frame definition differs from [39]. In this paper the tangent frame is identical to the tangent plane coordinates that is defined in reference [40].

In this section, the INS navigation equations are resolved in the tangent frame. Firstly, The GPS solution, expressed in earth geodetic, is converted to the tangent frame to achieve compatibility between the GPS and INS data. Hence, the required coordinate systems conversions

[DOI: 10.52547/jocee.1.1.49]

are presented. Secondly, the inertial navigation algorithm is expressed relative to the tangent frame; the attitude algorithm uses the quaternions approach, then, the velocity/position algorithm is achieved.

A. Transformation position and velocity vectors from geodetic frame to tangent frame

Transformation position and velocity vectors from geodetic frame to tangent frame

The GPS output is defined in the geodetic frame (g-frame) in terms of longitude, latitude, and height (or altitude). g-frame is a coordinate frame fixed to the earth's surface, based on the WGS 84 ellipsoid model. The position vector transformation from the geodetic system to the ECEF coordinate system is an intermediate step in converting the GPS position measurement to the local NED coordinate system or navigation frame (n-frame). The n-frame is based on the local horizon and its origin coincides with sensor frame. Given a point in the geodetic system, say $\mathbf{r}_g^e = [\varphi \ \lambda \ h]^T$, then GPS coordinates can be converted into ECEF frame using the following equations [3]:

$$\mathbf{r}_g^e = \begin{bmatrix} x_e \\ y_e \\ z_e \end{bmatrix} = \begin{bmatrix} (N+h)\cos\varphi\cos\lambda \\ (N+h)\cos\varphi\sin\lambda \\ [N(1-e^2)+h]\sin\lambda \end{bmatrix} \tag{1}$$

Since the origins of the e-frame and the n-frame are not identical, only difference vectors are converted. Then,

$$\mathbf{r}_g^n = \begin{bmatrix} x_n \\ y_n \\ z_n \end{bmatrix} = \mathbf{C}_e^n(\mathbf{r}_g^e - \mathbf{r}_{g_0}^e) = \mathbf{C}_e^n\left(\begin{bmatrix} x_e \\ y_e \\ z_e \end{bmatrix} - \begin{bmatrix} x_{e,0} \\ y_{e,0} \\ z_{e,0} \end{bmatrix}\right) \tag{2}$$

Where, the vector $\mathbf{r}_{g_0}^e$ is the position of the origin of the local NED frame.

$$\mathbf{r}_{g_0}^e = \begin{bmatrix} x_{e,0} \\ y_{e,0} \\ z_{e,0} \end{bmatrix} = \begin{bmatrix} (N_0+h_0)\cos\varphi_0\cos\lambda_0 \\ (N_0+h_0)\cos\varphi_0\sin\lambda_0 \\ [N_0(1-e^2)+h_0]\sin\lambda_0 \end{bmatrix} \tag{3}$$

$\mathbf{C}_e^n$ is the rotation matrix from the ECEF frame to the local NED frame, which is given by

$$\mathbf{C}_e^n = \begin{bmatrix} -\sin\varphi_0\cos\lambda_0 & -\sin\varphi_0\sin\lambda_0 & \cos\varphi_0 \\ -\sin\lambda_0 & \cos\lambda_0 & 0 \\ -\cos\varphi_0\cos\lambda_0 & -\cos\varphi_0\sin\lambda_0 & -\sin\varphi_0 \end{bmatrix} \tag{4}$$

The parameters λ_0 and φ_0 are the geodetic longitude and latitude corresponding to $\mathbf{r}_{e,0}$. On another hand, because the origin of the initial starting point for n-frame and n-frame are separated (not same), the transformation matrix $\mathbf{C}_n^{n_0}$ from n-frame to n_0-frame can be approximated to the following relation:

$$\mathbf{C}_n^{n_0} = \begin{bmatrix} 1 & (\lambda-\lambda_0)S_{\varphi_0} & -(\varphi-\varphi_0) \\ -(\lambda-\lambda_0)S_{\varphi_0} & 1 & -(\lambda-\lambda_0)C_{\varphi_0} \\ (\varphi-\varphi_0) & (\lambda-\lambda_0)C_{\varphi_0} & 1 \end{bmatrix} \tag{5}$$

The transformation matrix $\mathbf{C}_{n_0}^t$ from n0-frame to t-frame is given as follows.

$$\begin{aligned} \mathbf{C}_{n_0}^t &= \begin{bmatrix} \cos Az_0 & 0 & -\sin Az_0 \\ 0 & 1 & 0 \\ \sin Az_0 & 0 & \cos Az_0 \end{bmatrix}\begin{bmatrix} 1 & 0 & 0 \\ 0 & 0 & -1 \\ 0 & 1 & 0 \end{bmatrix} \\ &= \begin{bmatrix} \cos Az_0 & -\sin Az_0 & 0 \\ 0 & 0 & -1 \\ \sin Az_0 & \cos Az_0 & 0 \end{bmatrix} \end{aligned} \tag{6}$$

Where, the angle Az_0 is the vehicle azimuth at initial time t0. Therefore,

$$\mathbf{r}_g^t = \mathbf{C}_{n_0}^t\mathbf{C}_n^{n_0}\mathbf{C}_e^n(\mathbf{r}_g^e - \mathbf{r}_{g_0}^e) = \mathbf{C}_n^t\mathbf{C}_e^n(\mathbf{r}_g^e - \mathbf{r}_{g_0}^e) \tag{7}$$

where,

$$\mathbf{C}_n^t = \begin{bmatrix} c_{11} & c_{12} & c_{13} \\ -(\varphi-\varphi_0) & -(\lambda-\lambda_0)C_{\varphi_0} & -1 \\ -c_{12} & c_{11} & c_{33} \end{bmatrix}$$

$$\begin{aligned} c_{11} &= C_{Az_0} + (\lambda-\lambda_0)S_{\varphi_0}S_{Az_0} \\ c_{12} &= -S_{Az_0} + (\lambda-\lambda_0)S_{\varphi_0}C_{Az_0} \\ c_{13} &= -(\varphi-\varphi_0)C_{Az_0} + (\lambda-\lambda_0)C_{\varphi_0}S_{Az_0} \\ c_{33} &= -(\varphi-\varphi_0)S_{Az_0} - (\lambda-\lambda_0)C_{\varphi_0}C_{Az_0} \end{aligned} \tag{8}$$

The GPS gives the velocity of the carrier observed on the earth frame, which is different from the velocity observed in the tangent frame. The relations between them are derived in the following equations:

$$\mathbf{v}_t^t = \mathbf{v}_e^t + \boldsymbol{\omega}_{te}^t \times \mathbf{r}_g^t = \mathbf{v}_e^t \tag{9}$$

The vector $\boldsymbol{\omega}_{tb}^b$ is angular rate of the body (vehicle) frame relative to the t-frame, resolved in the body $\mathbf{v}^t = \mathbf{C}_e^t\mathbf{v}^e$. Because $\mathbf{v}^t$ is the velocity of the vehicle relative to the tangent frame, then equation (9) is the velocity correction formula, written in the form of components in the tangent coordinate system. Having explained the coordinate system, the next step is to represent the vehicle system relative to these frames. Note that the gyro data need to be integrated only once for determining the transformation matrix $\mathbf{C}_e^t$, but the (transformed) accelerometer measurements have to be integrated twice for position determination. These integrations lead to the accumulation of measurement errors over time experienced in every type of INS.

[DOI: 10.52547/jocee.1.1.49]

B. Navigation Equations in tangent frame

The inertial navigation equations are a set of differential equations, which relates the inertial quantities measured within the inertial frame to the navigation quantities in the t-frame.

1. Attitude Equations with Quaternion Algorithm

The quaternion differential equation provides a relation between the input angular rates and the attitude quaternion and it can be expressed in matrix form

$$\dot{\mathbf{q}} = \frac{1}{2}[\boldsymbol{\omega}_b \otimes]\mathbf{q} = \frac{1}{2}[\mathbf{q}\otimes]\boldsymbol{\omega} \tag{10}$$

where $\otimes$ represents the quaternion product between two quaternions as in [52], and $\boldsymbol{\omega}_b = \left[0, \omega_x, \omega_y, \omega_z\right]^T$ is the quaternion form of the angular rate (vector in three-dimensional space can be regarded as a quaternion with zero scalar). To solve equation (10), a similar method to that used in the DCM can be applied. That is applying the integration factor method, using the rotation vector for the angle integration during the update interval. Therefore,

$$\mathbf{q}(t) = \left[(\cos(0.5\Delta\theta)\mathbf{I} + \frac{\sin(0.5\Delta\theta)}{\Delta\theta}\left[\Delta\boldsymbol{\theta}\otimes\right]\right]\mathbf{q}(0) \tag{11}$$

where $\mathbf{I}$ is the matrix form of the unit quaternion, [1 0 0 0]^T, and $\left[\Delta\boldsymbol{\theta}\otimes\right]$ is for the quaternion of the rotation vector,

$$\left[\Delta\boldsymbol{\theta}\otimes\right] = \begin{bmatrix} 0 & -\Delta\theta_x & -\Delta\theta_y & -\Delta\theta_z \\ \Delta\theta_x & 0 & \Delta\theta_z & -\Delta\theta_y \\ \Delta\theta_y & -\Delta\theta_z & 0 & \Delta\theta_x \\ \Delta\theta_z & \Delta\theta_y & -\Delta\theta_x & 0 \end{bmatrix} \tag{12}$$

$$\Delta\theta_x = \omega_x d\tau,\ \Delta\theta_y = \omega_y d\tau,\ \Delta\theta_z = \omega_z d\tau$$

$$\Delta\theta = \sqrt{(\Delta\theta_x)^2 + (\Delta\theta_y)^2 + (\Delta\theta_z)^2}$$

To preserve the normality, the computed quaternion should be periodically normalized by dividing the quaternion $\mathbf{q}(k+1)$ by its magnitude $\left\|\mathbf{q}(k+1)\right\|$. With the initial conditions at lift-off, the quaternion parameters can be propagated using equation (11). As done for the Euler attitude angles. Using the instantaneous quaternion parameters, the $\mathbf{C}_b^t$ matrix is computed as

$$\mathbf{C}_b^t = \begin{bmatrix} q_0^2 + q_1^2 - q_2^2 - q_3^2 & 2(q_1q_2 - q_0q_3) & 2(q_1q_3 + q_0q_2) \\ 2(q_1q_2 + q_0q_3) & q_0^2 - q_1^2 + q_2^2 - q_3^2 & 2(q_3q_2 - q_0q_1) \\ 2(q_1q_3 - q_0q_2) & 2(q_3q_2 + q_0q_1) & q_0^2 - q_1^2 - q_2^2 + q_3^2 \end{bmatrix} \tag{13}$$

2. Velocity and Position Equations

The t-frame is assumed to be fixed relative to the center of the earth then, the rate velocity of the earth and t- frame system is equivalent, therefore:

$$\boldsymbol{\omega}_{et}^t = 0, \quad \Rightarrow \quad \boldsymbol{\omega}_{ie}^t = \boldsymbol{\omega}_{it}^t \tag{14}$$

For navigation in t-frame, the gravitational acceleration thus computed in ECI frame can be transformed to t-frame, by using the transformation matrix $\mathbf{C}_i^t$ as shown below:

$$\dot{\mathbf{v}}^t = \mathbf{C}_b^t\mathbf{f}^b + \mathbf{g}^t - 2\boldsymbol{\omega}_{ie}^t \times \mathbf{v}^t \tag{15}$$

where $\mathbf{f}^b$ represents the specific force acceleration, $\boldsymbol{\omega}_{ie}^t = \boldsymbol{\omega}_0^t = \mathbf{C}_i^t\boldsymbol{\omega}_{ie}^i$. In summary, the continuous-time navigation equations in the t-frame are:

$$\begin{aligned} \dot{\mathbf{r}}^t &= \mathbf{v}^t \\ \dot{\mathbf{v}}^t &= \mathbf{C}_b^t\mathbf{f}^b + \mathbf{g}^t - 2\boldsymbol{\omega}_0^t \times \mathbf{v}^t \\ \dot{\mathbf{C}}_b^t &= \mathbf{C}_b^t\left[\boldsymbol{\omega}_{ib}^b \times\right] - \left[\boldsymbol{\omega}_0^t \times\right] \end{aligned} \tag{16}$$

where the matrix $\mathbf{C}_b^t$ is a direction cosine matrix used to transform the measured specific force vector to t-frame. The matrix $\left[\boldsymbol{\omega}_{tb}^b \times\right]$ is the skew symmetric form of $\boldsymbol{\omega}_{tb}^b$ the body rate relative to t- frame.

$$\boldsymbol{\omega}_{tb}^b = \boldsymbol{\omega}_{ib}^b - \mathbf{C}_t^b\boldsymbol{\omega}_{ie}^t \tag{17}$$

A block diagram representation of the t-frame mechanization is shown in Fig. 2.

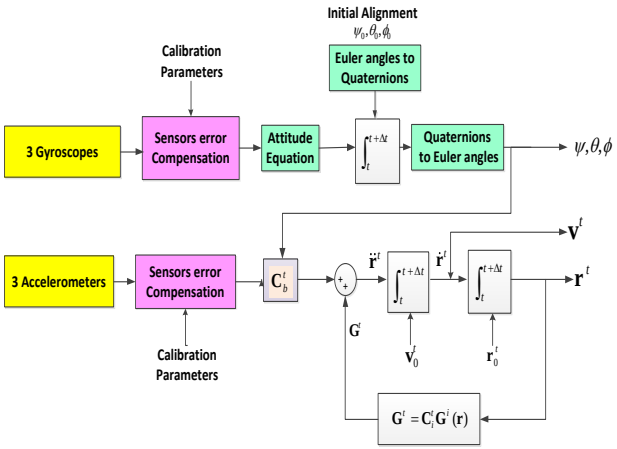

Fig. 2. Navigation computation in t-frame

C. Errors Model in Tangent frame

The errors that require to be estimated include misalignment attitude, position errors, velocity errors, and sensor uncertainty errors. They are defined as the deviations of the computed values from the true values. The perturbation method is used to linearize the nonlinear system differential equations. The errors in the position, velocity and attitude are defined as the estimated quantity

[DOI: 10.52547/jocee.1.1.49]

minus the true quantity as follows:

$$\begin{aligned}\delta\dot{\mathbf{r}}^t &= \delta\mathbf{v}^t\\ \delta\dot{\mathbf{v}}^t &= -\mathbf{E}^t\mathbf{f}^t - 2\boldsymbol{\omega}_{it}^t\times\delta\mathbf{v}^t + \mathbf{C}_b^t\delta\mathbf{f}^b + \delta\mathbf{g}^t\\ \dot{\boldsymbol{\varepsilon}}^t &= -\mathbf{C}_b^t\delta\boldsymbol{\omega}_{ib}^b - \left[\boldsymbol{\omega}_{it}^t\times\right]\boldsymbol{\varepsilon}^t\end{aligned} \tag{18}$$

or

$$\begin{bmatrix}\delta\dot{\mathbf{r}}^t\\ \delta\dot{\mathbf{v}}^t\\ \dot{\boldsymbol{\varepsilon}}^t\end{bmatrix} = \begin{bmatrix}0_{3\times3} & \mathbf{I}_{3\times3} & 0_{3\times3}\\ 0_{3\times3} & -2\left[\boldsymbol{\omega}_{it}^t\times\right] & -\left[\mathbf{f}^t\times\right]\\ 0_{3\times3} & 0_{3\times3} & -\left[\boldsymbol{\omega}_{it}^t\times\right]\end{bmatrix}\begin{bmatrix}\delta\mathbf{r}^t\\ \delta\mathbf{v}^t\\ \boldsymbol{\varepsilon}^t\end{bmatrix} + \begin{bmatrix}0_{3\times3} & 0_{3\times3}\\ \mathbf{C}_b^t & 0_{3\times3}\\ 0_{3\times3} & -\mathbf{C}_b^t\end{bmatrix}\begin{bmatrix}\delta\mathbf{f}^b\\ \delta\boldsymbol{\omega}_{ib}^b\end{bmatrix} \tag{19}$$

The INS error equation forms a basis to formulate the indirect filter in this paper, where

$$\boldsymbol{\omega}_{it}^t = \mathbf{C}_i^t\boldsymbol{\omega}_{ie}^i = \begin{bmatrix}\omega_e\cos(Az_0)\cos(\varphi_0)\\ \omega_e\sin(\varphi_0)\\ -\omega_e\sin(Az_0)\cos(\varphi_0)\end{bmatrix} \tag{20}$$

D. Modified INS Error Equations for IP-EKF

Equations (16) are linearized to obtain a linear state error model using the perturbations analysis method [28]. Position error, velocity error, and attitude error are expressed as follows, $\delta\mathbf{r}^t = \mathbf{r}^t - \hat{\mathbf{r}}^t$, $\delta\mathbf{v}^t = \mathbf{v}^t - \hat{\mathbf{v}}^t$, $\delta\mathbf{f}^b = \Delta\hat{\mathbf{f}}^b - \Delta\mathbf{f}^b$, and $\delta\boldsymbol{\omega}_{ib}^b = \Delta\hat{\boldsymbol{\omega}}_{ib}^b - \Delta\boldsymbol{\omega}_{ib}^b$. Where δ is the error of the corresponding quantity. Using the perturbations method the state error equation is expressed via:

$$\delta\dot{\mathbf{x}}(t) = \mathbf{F}(t)\delta\mathbf{x}(t) + \mathbf{m}(t) + \mathbf{w}(t) \tag{21}$$

The error state vector contains 9 parameters as follows, $\delta\mathbf{x} = \left[\delta\mathbf{r}^t\ \delta\mathbf{v}^t\ \boldsymbol{\varepsilon}^t\right]^T$, where $\delta\mathbf{r}^t$ is the position error vector (m), $\delta\mathbf{v}^t$ is the velocity error vector (m/sec) and $\boldsymbol{\varepsilon}^t$ is the attitude error vector (rad). The vector $\boldsymbol{\varepsilon}^t$ contains the small-angle between the earth frame and the computed earth frame. In addition, the vector $\mathbf{m}(t)$ is the unknown model error to be predicted in the proposed incremental predictive algorithm, and the transition matrix $\mathbf{F}(t)$ is determined as follows:

$$\mathbf{F}(t) = \begin{bmatrix}\mathbf{0}_{3\times3} & \mathbf{I}_{3\times3} & \mathbf{0}_{3\times3}\\ \mathbf{0}_{3\times3} & -2\left[\boldsymbol{\omega}_{it}^t\times\right] & -\left[\mathbf{f}^t\times\right]\\ \mathbf{0}_{3\times3} & \mathbf{0}_{3\times3} & -\left[\boldsymbol{\omega}_{it}^t\times\right]\end{bmatrix} \tag{22}$$

The $\mathbf{0}_{3\times3}$ is the matrix which all its elements are zero, $\mathbf{I}_{3\times3}$ is the unite matrix. Further, $\left[\mathbf{f}^t\times\right]$ is the skew-symmetric matrix form of $\mathbf{f}^t = \mathbf{C}_b^t\mathbf{f}^b$; the input specific force acceleration in the t-frame. The matrix $\left[\boldsymbol{\omega}_{it}^t\times\right]$ is the skew-symmetric matrix form of $\boldsymbol{\omega}_{it}^t$, the earth rate resolved in the t-frame. To formulate the discrete GIP-KF, it is necessary to express (21) in discrete form. Therefore,

$$\delta\mathbf{x}_{k+1} = \mathbf{F}_k\delta\mathbf{x}_k + \mathbf{m}_k + \mathbf{w}_k \tag{23}$$

where the vector $\delta\mathbf{x}_k$ is the state error at time k, $\mathbf{m}_k$ is the model error vector, $\mathbf{w}_k$ is additive system noise, and $\mathbf{F}_k$ is the state error transition matrix. For small time interval ($dt = t_{k+1} - t_k$), the matrix $\mathbf{F}_k$ is expressed in term of F(t) as follows: $\mathbf{F}_k = \exp(\mathbf{F}(t)dt) \approx \mathbf{I} + \mathbf{F}(t)dt$. It is evident that the cost function (32) is well posed because it uses the unknown incremental model error $\Delta\hat{\mathbf{m}}_k$ rather than $\hat{\mathbf{m}}_k$ with nonzero mean. The proposed cost function is unbiased with $\delta\mathbf{y}_{k+1} = \delta\hat{\mathbf{y}}_{k+1}$ and $\Delta\hat{\mathbf{m}}_k = 0$.

At t_{k-1} equation (23) gives $\delta\mathbf{x}_k = \mathbf{F}_{k-1}\delta\mathbf{x}_{k-1} + \mathbf{m}_{k-1} + \mathbf{w}_{k-1}$ and by subtraction this equation from equation (23), incremental form of the error model is obtained by

$\Delta(\delta\mathbf{x}_{k+1}) = \mathbf{F}_k\delta\mathbf{x}_k - \mathbf{F}_{k-1}\delta\mathbf{x}_{k-1} + \Delta\mathbf{m}_k + \Delta\mathbf{w}_k$,

where $\Delta\mathbf{w}_k = \mathbf{w}_k - \mathbf{w}_{k-1}$, $\Delta(\delta\mathbf{x}_{k+1}) = \delta\mathbf{x}_{k+1} - \delta\mathbf{x}_k$, and $\Delta\mathbf{m}_k = \mathbf{m}_k - \mathbf{m}_{k-1}$. Therefore,

$$\delta\mathbf{x}_{k+1} = (\mathbf{I} + \mathbf{F}_k)\delta\mathbf{x}_k - \mathbf{F}_{k-1}\delta\mathbf{x}_{k-1} + \Delta\mathbf{m}_k + \Delta\mathbf{w}_k \tag{24}$$

Equation (24) contains the model error changes (increments) $\Delta\mathbf{m}_k$. The term Δ in (24) indicates to presence of integrals in the system. This eliminates the static error in the estimate. In (24), future state error (at t_{k+1}) is predicted according to state error at the moments t_k and t_{k-1}. The measurement model observes the differences of estimated position and velocity error between INS and GPS. The observation equation for the GIP-KF algorithm is written as follows:

$$\delta\mathbf{y}_{k+1} = \mathbf{H}\delta\mathbf{x}_{k+1} + \mathbf{v}_{k+1} \tag{25}$$

where the vector error $\delta\mathbf{y}_{k+1}$ express the vector measurement at time t_{k+1}. The vector $\delta\mathbf{x}_{k+1}$ is the state error. The measurement noise $\mathbf{v}_{k+1}$ is Gaussian white noises with zero mean and covariance matrix $\mathbf{R}_{v,k+1}$. The measurement matrix $\mathbf{H}$ is as follows:

$$\mathbf{H} = \begin{bmatrix}\mathbf{I}_{3\times3} & \mathbf{0}_{3\times3} & \mathbf{0}_{3\times3}\\ \mathbf{0}_{3\times3} & \mathbf{I}_{3\times3} & \mathbf{0}_{3\times3}\end{bmatrix} \tag{26}$$

It is assumed that, the process noise $\Delta\mathbf{w}_k$ and measurement noise $\mathbf{v}_{k+1}$ are uncorrelated, zero-mean white-noise processes with known symmetric positive

[DOI: 10.52547/jocee.1.1.49]

semi-definite covariance matrices $\mathbf{Q}_{\Delta,k}$ and $\mathbf{R}_{v,k+1}$, respectively. The initial random state error, $\delta\mathbf{x}_0$ has a mean $\delta\hat{\mathbf{x}}_0$ and covariance matrix $\mathbf{P}_0$. Therefore, the optimal estimate of the state error $\delta\mathbf{x}_{k+1}$, which is denoted by $\delta\hat{\mathbf{x}}_{k+1}$, that minimizes the expectation of the squared-error cost function $E(\left\|\delta\mathbf{x}_{k+1}-\delta\hat{\mathbf{x}}_{k+1}\right\|^2)$. The solution is the following predicted state error:

$$\begin{aligned}\delta\hat{\mathbf{x}}_{k+1/k} &= (\mathbf{I}+\mathbf{F}_k)\delta\hat{\mathbf{x}}_k - \mathbf{F}_{k-1}\delta\hat{\mathbf{x}}_{k-1} + \Delta\hat{\mathbf{m}}_k \\ \delta\hat{\mathbf{y}}_{k+1/k} &= \mathbf{H}\delta\hat{\mathbf{x}}_{k+1}\end{aligned} \tag{27}$$

where the vector $\delta\hat{\mathrm{x}}\in\mathbb{R}^{n\times1}$, $\delta\hat{\mathbf{y}}\in\mathbb{R}^{m\times1}$, $\Delta\hat{\mathrm{m}}\in\mathbb{R}^{n\times1}$, $\mathrm{F}\in\mathbb{R}^{n\times n}$, and $\mathrm{H}\in\mathbb{R}^{m\times n}$. In (27), the proposed filter uses both current and previous states. The unknown model error input $\Delta\hat{\mathrm{m}}_k$ is predicted using the proposed approach as described in the next section.

III. Proposed Filtering Algorithms Derivation

This section demonstrates the strategy of the GIP_KF algorithm to estimate the unknown model error $\hat{\mathbf{m}}_k$. The incremental form of the state space that is modelled in equation (23) can be written as follows:

$$\Delta\hat{\mathbf{x}}_{k+1/k} = \Delta\mathbf{F}_k\Delta\hat{\mathbf{x}}_k + \Delta\mathbf{m}_k \tag{28}$$

where $\Delta\hat{\mathbf{x}}_{k+1/k} = \delta\hat{\mathbf{x}}_{k+1/k} - \delta\hat{\mathbf{x}}_k$, $\Delta\hat{\mathbf{x}}_k = \delta\hat{\mathbf{x}}_k - \delta\hat{\mathbf{x}}_{k-1}$, $\Delta\hat{\mathbf{m}}_k = \hat{\mathbf{m}}_k - \hat{\mathbf{m}}_{k-1}$ and $\Delta\mathbf{F}_k = \mathbf{F}_k - \mathbf{F}_{k-1}$. By writing this form we can get the model error signal changes $\Delta\mathbf{m}_k$. In fact, when we add Δ to the above equations, it means adding integrals to the system. This eliminates the static error in the estimate. By combining the above equations, the equation one step ahead is obtained as follows:

$$\hat{\mathbf{x}}_{k+1/k} = (\mathbf{I}+\mathbf{F}_k)\hat{\mathbf{x}}_k - \mathbf{F}_{k-1}\hat{\mathbf{x}}_{k-1} + \Delta\hat{\mathbf{m}}_k \tag{29}$$

where $\mathbf{I}$ is the unit matrix. In this equation, states are calculated in moment *k+1* according to moments *k* and *k-1*. The minus sign of this relation is actually a kind of derivation of states in this method. The prediction of system outputs can be stated as the following compact equation:

$$\mathbf{y}_{k+1/k} = \mathbf{H}_{k+1}(\mathbf{I}+\mathbf{F}_k)\hat{\mathbf{x}}_k - \mathbf{H}_{k+1}\mathbf{F}_{k-1}\hat{\mathbf{x}}_{k-1} + \mathbf{H}_{k+1}\Delta\hat{\mathbf{m}}_k \tag{30}$$

where $\hat{\mathbf{x}},\Delta\hat{\mathbf{m}}\in\mathbb{R}^{n\times1}$, $\hat{\mathbf{y}}\in\mathbb{R}^{m\times1}$, $\mathbf{F}\in\mathbb{R}^{n\times n}$, and $\mathbf{H}\in\mathbb{R}^{m\times n}$. Equation (30) can be rewritten as follows:

$$\mathbf{y}_{k+1/k} = \mathbf{H}_1\hat{\mathbf{x}}_k - \mathbf{H}_2\hat{\mathbf{x}}_{k-1} + \mathbf{H}_3\Delta\hat{\mathbf{m}}_k \tag{31}$$

where, $\mathbf{H}_1 = \mathbf{H}_{k+1}(\mathbf{I}+\mathbf{F}_k)$, $\mathbf{H}_2 = \mathbf{H}_{k+1}\mathbf{F}_{k-1}$ and $\mathbf{H}_3 = \mathbf{H}_{k+1}$.

A. Definition and minimization of the cost function

To achieve the optimal solution of $\Delta\hat{\mathbf{m}}_k$, a cost function consisting of the measurement residual term and the model error increment term is defined as follows:

$$\min_{\Delta\hat{\mathbf{m}}_k}\mathbf{J} = \left(\mathbf{y}_{k+1}-\hat{\mathbf{y}}_{k+1}\right)^T\mathbf{R}_{k+1}^y\left(\mathbf{y}_{k+1}-\hat{\mathbf{y}}_{k+1}\right) + \Delta\hat{\mathbf{m}}_k^T\mathbf{R}_k^m\Delta\hat{\mathbf{m}}_k \tag{32}$$

where y_{k+1} is output reference at time *k+1*, the positive semi definite matrices $\mathbf{R}_k^m$ and $\mathbf{R}_{k+1}^y$ are weighting matrices of reference tracking error and increment input moves. These matrices are the filter tuning parameters. When $\mathbf{R}_k^m$ decreases, more model error is added to correct the model, so that the estimates more closely follow the measurements. When $\mathbf{R}_k^m$ increases, less model error is added, then the estimates more closely follow the propagated model. Finding optimal increment input which minimizes quadratic cost function (32) represents optimization problem, in the case when there are no constraints, the optimal increment input can be found as an analytic solution as follows:

$$\Delta\hat{\mathbf{m}}_k^* = \mathbf{K}_k^{GIPKF}\left(\mathbf{y}_{k+1} - \mathbf{H}_1\hat{\mathbf{x}}_k + \mathbf{H}_2\hat{\mathbf{x}}_{k-1}\right) \tag{33}$$

where the gain of GIP_KF filter is:

$$\mathbf{K}_k^{GIPKF} = (\mathbf{H}_3^T\mathbf{R}_{k+1}^y\mathbf{H}_3 + \mathbf{R}_k^m)^{-1}\mathbf{H}_3^T\mathbf{R}_{k+1}^y\left(\mathbf{y}_{k+1} - \mathbf{H}_1\hat{\mathbf{x}}_k + \mathbf{H}_2\hat{\mathbf{x}}_{k-1}\right) \tag{34}$$

As shown in equations (29) and (34), the proposed filter uses both current and previous states rather than the current state to predict the unknown model error input and the current and previous states create the weighted difference term in the optimal solution of the model error.

B. GIP-KF Prediction and correction loop

The optimal increment model error is calculated from equation (29). The predicted error state estimate at stage $k+1$, given the measurements up to stage *k*+1, can be given by:

$$\begin{cases}\hat{\mathbf{x}}_{k+1/k} = (\mathbf{I}+\mathbf{F}_k)\hat{\mathbf{x}}_k - \mathbf{F}_{k-1}\hat{\mathbf{x}}_{k-1} + \Delta\hat{\mathbf{m}}_k \\ \hat{\mathbf{y}}_{k+1} = \mathbf{H}_{k+1}\hat{\mathbf{x}}_{k+1/k} \\ \mathbf{P}_{k+1/k} = \mathbf{F}_k\mathbf{P}_k\mathbf{F}_k^T + \mathbf{Q}_k\end{cases} \tag{35}$$

$$\begin{cases}\mathbf{K}_{k+1} = \mathbf{P}_{k+1/k}\mathbf{H}_{k+1}^T\left[\mathbf{H}_{k+1}\mathbf{P}_{k+1/k}\mathbf{H}_{k+1}^T + \mathbf{R}_{k+1}\right]^{-1} \\ \hat{\mathbf{x}}_{k+1} = \hat{\mathbf{x}}_{k+1/k} + \mathbf{K}_{k+1}\left[\mathbf{y}_{k+1} - \hat{\mathbf{y}}_{k+1}\right] \\ \mathbf{P}_{k+1} = \left[\mathbf{I} - \mathbf{K}_{k+1}\mathbf{H}_{k+1}\right]\mathbf{P}_{k+1/k}\end{cases} \tag{36}$$

where $\mathbf{K}_{k+1}$ is the Kalman gain, which defines the updating weight between new measurements and predictions from the system dynamic model. The innovation sequence is defined as $\left[\mathbf{y}_{k+1} - \hat{\mathbf{y}}_{k+1}\right]$. Equations (32) through (34), present the GIP-KF method of estimating the incremental model error and the perturbation part of the state. The algorithm has automatic repair statistical characteristics of model error that improve filtering precision. After applying the first model error move of optimal sequence to system, new output is measured and new optimal model error sequence $\Delta\hat{\mathbf{m}}_k$ is computed. The simplified GIPKF framework algorithm is illustrated in Fig. 3.

[DOI: 10.52547/jocee.1.1.49]

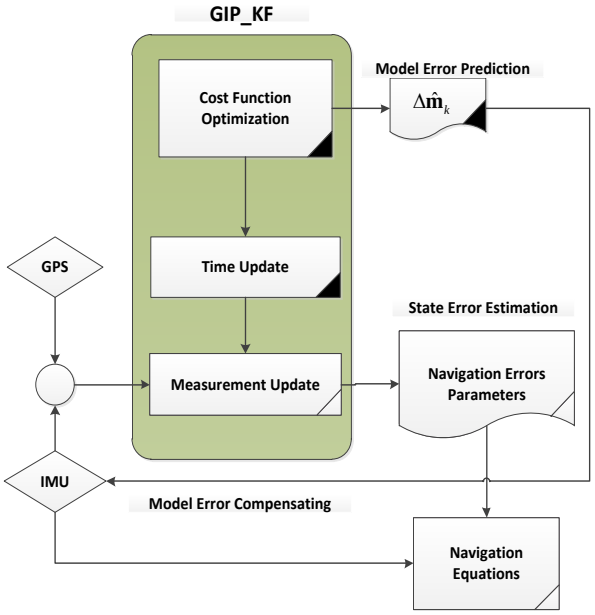

Fig. 3. The simplified GIP_KF framework algorithm for INS/GPS integration

IV. Simulation Results

In this section, a real car test for the verification of the performance of the GIP_KF proposed in the research will be investigated. The prototype of a real-time integrated system consists of an IMU type AIDS16488A which is integrated with a GPS receiver type GARMAIN, and an on-board computer. Fig. 4 shows the hardware that are used in the test, in order to implement the navigation equations.

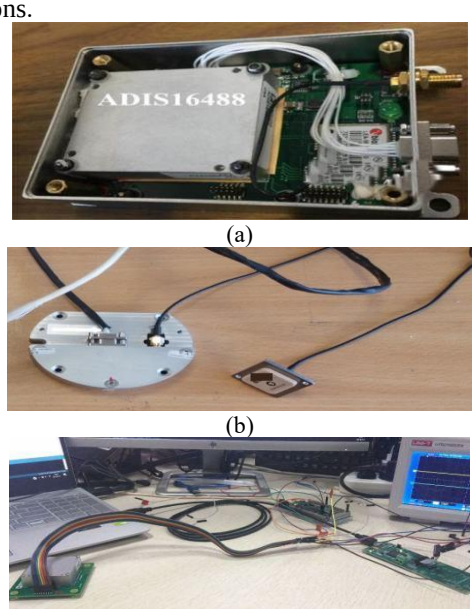

(a)

(b)

(c)

Fig. 4. The hardware adopted in the experiment

A. Analysis of the results

The performance is analyzed during GPS outages using the values of the estimated navigation parameters (…, position, velocity, attitude, …) of the proposed IPKF method and the extended Kalman filter. The robustness of the navigation system during GPS outages is tested with three duration of GPS outages of 10, 11, and 22 seconds as is illustrated in Fig. 5.

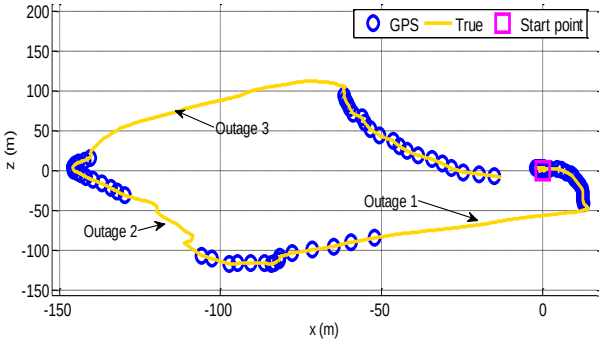

Fig. 5. The tested trajectory

Fig. 6 shows a significant reduction in position error growth during the GPS outages when the proposed filter is used. This figure indicates that the estimated positions by EKF are increased rapidly when the GPS signal is not available. According to the above results of the trajectory, the filtering accuracy of the GIP-KF is better than that of the EKF. When the GPS has an outage, the EKF immediately diverges. This proves that when an outage occurs, compared with the EKF, the IP-EKF has strong robustness, and it predicts the model error in each time step. In this case, the proposed filter has higher accuracy for INS/GPS online correction when the model error is unknown.

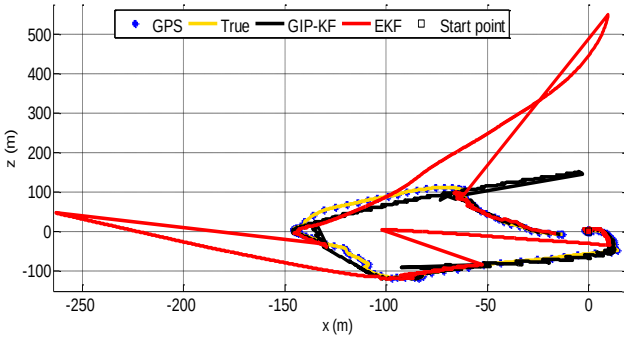

Fig. 6. The estimated trajectory by GIP-KF and EKF

In Fig. 7, it can be seen that IP-EKF results are more accurate than the extended Kalman filtering for position errors of horizontal plane. The EKF gives an error magnitude of about 455 m, after 22 sec (outage 3), while the error magnitude of the proposed filter is around 82 m, after 22 sec (outage 3). The EKF estimation performance in both horizontal directions is highly degraded compared to the GIP-KF estimation performance during the third GPS outage. Fig. 7 shows about 80% reduction in position errors during GPS outages in the case of using

[DOI: 10.52547/jocee.1.1.49]

the GIP-KF.

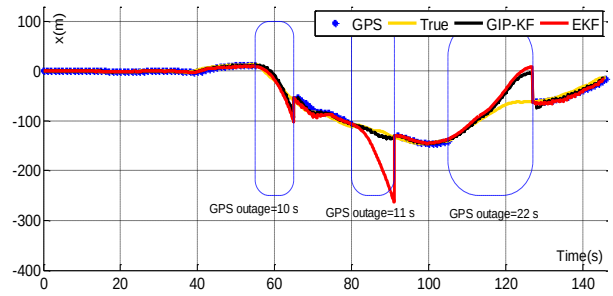

(a)

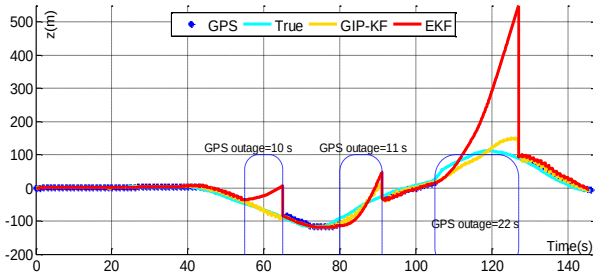

(b)

Fig. 7. The estimated horizontal (x and z) position for the tested trajectory by GIP-KF and EKF

The horizontal navigation errors and vehicle trajectory in terms of the root mean square error (RMSE) and the mean error of vertical axis are given in Table.2. The calculated RMSE for the horizontal errors and the mean vertical error demonstrate good performance of the proposed filter relative to the tradition EKF (15 states).

TABLE I
THE HORIZONTAL NAVIGATION ERRORS

	RMS of horizontal position error (m)	
Algorithm	IP-EKF	EKF
Total trajectory with 3 outages	15.15	79.63

The case when observing the linear velocities of vehicle from IP-EKF and EKF are also shown in Fig. 8. The comparison of the results shows that in the case of IP-EKF, the velocity error growth during the GPS outage is decreased.

It is clear from the previous figures that the IP-EKF approach is more accurate and robust than the traditional EKF witch not converge rapidly after the long GPS outage (the third case when the GPS is blocked for 22 sec.), while the new filter converges to the true velocities more rapidly.

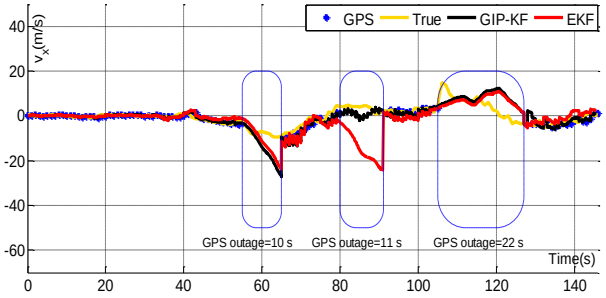

(a)

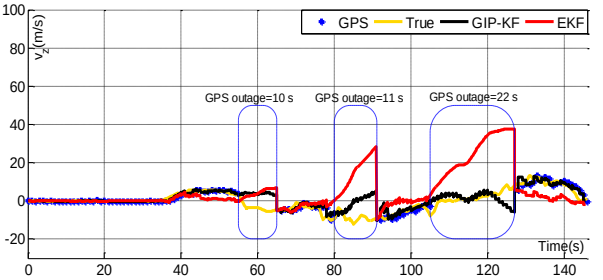

(b)

Fig. 8. The estimated x and z velocity for the tested trajectory by GIP-KF and EKF

The quality of the information provided by the sensors in the navigation system has a direct influence on the overall system's performance. The sensors model error information play an equivalent role in the estimation of the vehicle state. It is clear, that navigation system performance is enhanced by compensating for model error in real-time. Fig. 9 shows the estimated biases for the accelerometers and the gyroscopes using GIP-KF and EKF.

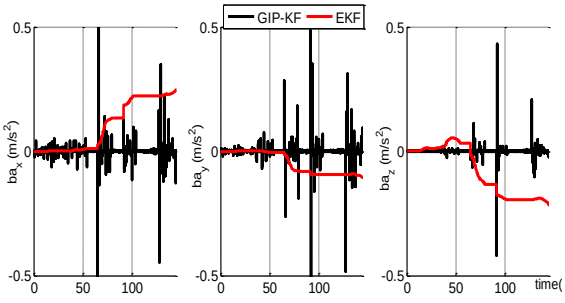

(a)

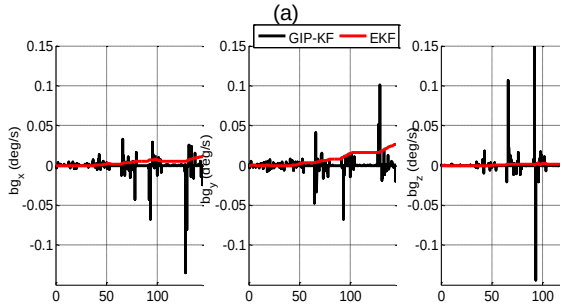

(b)

Fig. 9. The estimated biases for the accelerometers (a) and gyroscopes (b) by IP-EKF and EKF

[DOI: 10.52547/jocee.1.1.49]

Fig. 10 presents the estimated attitude for IP-EKF and EKF; the results show that the GPS outages not influence the attitude estimate.

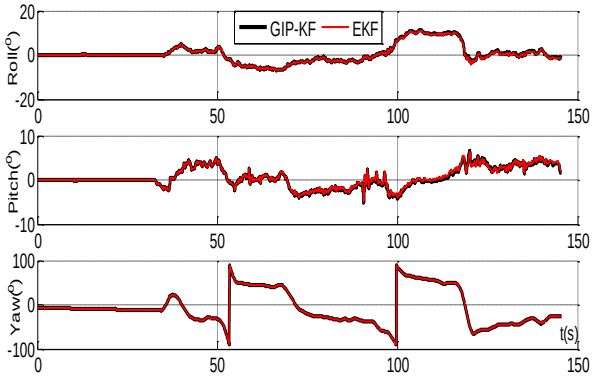

Fig. 10. The estimated attitude by IP-EKF and EKF

In this section, the GIP-KF was validated during a real experiment for the INS/GPS integrated navigation and with simulation of a car test, which demonstrates the effectiveness of the proposed GIP-KF in terms of positioning accuracy compared to the EKF.

B. Analysis of the performance of the proposed method

The validity of the proposed filter is verified using loosely coupled MEMS INS/GPS experimental data. To realizes and analyze the performance of the proposed approach, the IP-EKF is compared to EKF. The integration algorithm uses an augmented model of EKF with 15 states and IP-EKF with only 9 states. The results demonstrate that the new filter is more robust to GPS outages than EKF. The paper implements the approximate calculations of the number of floating-point operations per second (FLOPS) performed for a given algorithm. As a result, 30800 FLOPS are needed in each cycle, of EKF algorithm, while GIP-KF requires only 15050 FLOPS. Therefore, the GIP_KF decreases the computational cost to 50% and increases the accuracy of the horizontal position error by an amount of 81% comparing to EKF. Also, it improves the speed of estimation convergence comparing to EKF. Therefore, IP-EKF can be used in real-time, with high reliability and accuracy.

V. CONCLUSIONS

This paper presents a novel incremental predictive approach to increase the performance of the extended Kalman filter for integrated INS/GPS when the GPS is blocked. Since the performance of the combined INS/GPS degrades during the GPS outage because of the remarkable model error of the MEMS-IMU, the conventional EKF may become unstable, and its convergence is not confirmed. Further, the degree of observability of some error states is inadequate due to the state's augmentation. The proposed algorithm predicts and compensates for the unknown model error of sensors by minimizing a quadratic cost function consisting of a measurement innovation and the incremental model error term.

The research demonstrates formulation, the deterministic full observability, stability, and convergence of the proposed filter. The test results of land-vehicle navigation validate the advantages of the presented method, which increases the position accuracy by an amount of 81% and it decreases the computational cost to 50% and improves the estimation performance This test is a for the integrated INS/GPS better than the traditional EKF.

REFERENCES

[1] A. Lawrence, Modern inertial technology: navigation, guidance, and control. Springer Science & Business Media, 2012.

[2] D. Titterton, J. L. Weston, and J. Weston, Strapdown inertial navigation technology. IET, 2004.

[3] L. Zhang, H. Yang, S. Zhang, H. Cai, and S. Qian, "Strapdown stellar-inertial guidance system for launch vehicle," Aerospace Science and Technology, vol. 33, no. 1, pp. 122-134, 2014.

[4] H.-m. Qian, L. Sun, J.-n. Cai, and Y. Peng, "A novel navigation method used in a ballistic missile," Measurement Science and Technology, vol. 24, no. 10, p. 105011, 2013.

[5] L. Yang, B. Li, and L. Ge, "A novel SINS/CNS integrated navigation algorithm used in a ballistic missile," Int. J. Secur. Appl, vol. 9, pp. 65-76, 2015.

[6] L. Zhang, Z. Zhai, L. He, P. Wen, and W. Niu, "Infrared-Inertial Navigation for Commercial Aircraft Precision Landing in Low Visibility and GPS-Denied Environments," Sensors, vol. 19, no. 2, p. 408, 2019.

[7] C. Zhang, T. Li, and C. Guo, "GPS/INS integration based on adaptive interacting multiple model," The Journal of Engineering, vol. 2019, no. 15, pp. 561-565, 2019.

[8] W. Wang et al., "Integrated navigation method based on inertial and geomagnetic information fusion," in Optical Sensing and Imaging Technologies and Applications, 2018, vol. 10846, p. 1084615: International Society for Optics and Photonics.

[9] Q. Dai, L. Sui, L. Wang, T. Zeng, and Y. Tian, "An efficiency algorithm on Gaussian mixture UKF for BDS/INS navigation system," Geodesy and Geodynamics, vol. 9, no. 2, pp. 169-174, 2018.

[10] Z. Gao, Y. Li, Y. Zhuang, H. Yang, Y. Pan, and H. Zhang, "Robust Kalman Filter Aided GEO/IGSO/GPS Raw-PPP/INS Tight Integration," Sensors, vol. 19, no. 2, p. 417, 2019.

[11] N. Ghahramani, M. A. Ashtiani, A. Mohammadi, and M. Fallah, "Adaptive Fusion of Inertial Navigation System and Tracking Radar Data," AUT

[DOI: 10.52547/jocee.1.1.49]

Journal of Elec trical Engineering, vol. 48, no. 2, pp. 81-92, 2016.

[12] X. Zhao, J. Li, X. Yan, and S. Ji, "Robust Adaptive Cubature Kalman Filter and Its Application to Ultra-Tightly Coupled SINS/GPS Navigation System," Sensors, vol. 18, no. 7, p. 2352, 2018.

[13] B. Hou, Z. He, D. Li, H. Zhou, and J. Wang, "Maximum correntropy unscented kalman filter for ballistic missile navigation system based on SINS/CNS deeply integrated mode," Sensors, vol. 18, no. 6, p. 1724, 2018.

[14] J. Pan, Z. Xiong, H. Zhao, F. Yu, and L. Wang, "SINS/GPS/CNS multi-integrated navigation system algorithm in launch inertial coordinate system and realization," Chin. Space Sci. Technol, vol. 35, pp. 9-16, 2015.

[15] R. E. Kalman, "A new approach to linear filtering and prediction problems," Journal of basic Engineering, vol. 82, no. 1, pp. 35-45, 1960.

[16] Y. Song and J. W. Grizzle, "The extended Kalman filter as a local asymptotic observer for nonlinear discrete-time systems," in 1992 American control conference, 1992, pp. 3365-3369: IEEE.

[17] N. A. Anbu and D. Jayaprasanth, "Integration of Inertial Navigation System with Global Positioning System using Extended Kalman Filter," in 2019 International Conference on Smart Systems and Inventive Technology (ICSSIT), 2019, pp. 789-794: IEEE.

[18] A. Doucet, N. J. Gordon, and V. Krishnamurthy, "Particle filters for state estimation of jump Markov linear systems," IEEE Transactions on signal processing, vol. 49, no. 3, pp. 613-624, 2001.

[19] K.-W. Chiang, INS/GPS integration using neural networks for land vehicular navigation applications (no. NR-04589 UMI). University of Calgary Canada, 2004.

[20] M. Aslinezhad, A. Malekijavan, and P. Abbasi, "ANN-assisted robust GPS/INS information fusion to bridge GPS outage," EURASIP Journal on Wireless Communications and Networking, vol. 2020, no. 1, pp. 1-18, 2020.

[21] E. F. Camacho and C. B. Alba, Model Predictive Control. Springer, 2013.

[22] W. Wei, S. Gao, Y. Zhong, C. Gu, and G. Hu, "Adaptive Square-Root Unscented Particle Filtering Algorithm for Dynamic Navigation," Sensors, vol. 18, no. 7, p. 2337, 2018.

[23] Y. Liu, X. Fan, C. Lv, J. Wu, L. Li, and D. Ding, "An innovative information fusion method with adaptive Kalman filter for integrated INS/GPS navigation of autonomous vehicles," Mechanical Systems and Signal Processing, vol. 100, pp. 605-616, 2018.

[24] J. Kim, S. Vaddi, P. Menon, and E. J. Ohlmeyer, "Comparison between nonlinear filtering techniques for spiraling ballistic missile state estimation," IEEE Transactions on Aerospace and Electronic Systems, vol. 48, no. 1, pp. 313-328, 2012.

[25] M. S. Arulampalam, S. Maskell, N. Gordon, and T. Clapp, "A tutorial on particle filters for online nonlinear/non-Gaussian Bayesian tracking," IEEE Transactions on signal processing, vol. 50, no. 2, pp. 174-188, 2002.

[26] B. F. La Scala, R. R. Bitmead, and M. R. James, "Conditions for stability of the extended Kalman filter and their application to the frequency tracking problem," Mathematics of Control, Signals and Systems, vol. 8, no. 1, pp. 1-26, 1995.

[27] H. Odéen and D. Parker, "Dynamical model parameter adjustments in model predictive filtering MR thermometry," Journal of therapeutic ultrasound, vol. 3, no. 1, p. P31, 2015.

[28] W. Qiuying, Z. Minghui, G. Zheng, and W. Hui, "Integrated navigation method using marine inertial navigation system and star sensor based on model predictive filtering," in 2018 IEEE/ION Position, Location and Navigation Symposium (PLANS), 2018, pp. 850-857: IEEE.

[29] L. Zhang, S. Qian, S. Zhang, and H. Cai, "Federated nonlinear predictive filtering for the gyroless attitude determination system," Advances in Space Research, vol. 58, no. 9, pp. 1671-1681, 2016.

[30] L. Cao, X. Chen, and A. K. Misra, "A novel unscented predictive filter for relative position and attitude estimation of satellite formation," Acta Astronautica, vol. 112, pp. 140-157, 2015.

[31] L. Cao and H. Li, "Norm-constrained predictive filtering for attitude estimation," Proceedings of the Institution of Mechanical Engineers, Part G: Journal of Aerospace Engineering, vol. 230, no. 10, pp. 2000-2006, 2016.

[32] J. Fang and X. Gong, "Predictive iterated Kalman filter for INS/GPS integration and its application to SAR motion compensation," IEEE Transactions on Instrumentation and Measurement, vol. 59, no. 4, pp. 909-915, 2009.

[33] M. Fathi, N. Ghahramani, M. A. Shahi Ashtiani, A. Mohammadi, and M. Fallah, "Incremental predictive Kalman filter for alignment of inertial navigation system," Proceedings of the Institution of Mechanical Engineers, Part G: Journal of Aerospace Engineering, p. 0954410018794324, 2018.

[34] A. Bose, K. Bhat, and T. Kurian, Fundamentals of navigation and inertial sensors. PHI Learning Pvt. Ltd., 2014.

[35] K. Chen, F. Shen, J. Zhou, and X. Wu, "Simulation platform for SINS/GPS integrated navigation system of hypersonic vehicles based on flight mechanics," Sensors, vol. 20, no. 18, p. 5418, 2020.

[36] K. Chen, F. Shen, J. Zhou, and X. Wu, "SINS/BDS Integrated Navigation for Hypersonic Boost-

[DOI: 10.52547/jocee.1.1.49]

Glide Vehicles in the Launch-Centered Inertial Frame," Mathematical Problems in Engineering, vol. 2020, 2020.

[37] K. Chen, S. Pei, F. Shen, and S. Liu, "Tightly Coupled Integrated Navigation Algorithm for Hypersonic Boost-Glide Vehicles in the LCEF Frame," Aerospace, vol. 8, no. 5, p. 124, 2021.

[38] K. Chen, J. Zhou, F.-Q. Shen, H.-Y. Sun, and H. Fan, "Hypersonic boost–glide vehicle strapdown inertial navigation system/global positioning system algorithm in a launch-centered earth-fixed frame," Aerospace Science and Technology, vol. 98, p. 105679, 2020.

[39] J. Farrell, Aided navigation: GPS with high rate sensors. McGraw-Hill, Inc., 2008.

[40] J. Gurley, "Inertial Guidance (GR Pitman, Jr," SIAM Review, vol. 5, no. 1, p. 81, 1963.

[DOI: 10.52547/jocee.1.1.49]